Spatial Light Modulators

M. Gostiaux Gabriel
M. Gabriel Gostiaux, Master of Science student, Institute of Optics, Palaiseau, 91 120, France
gabriel.gostiaux@institutoptique.fr

https:reacton-brew.com

Abstract: In this study, we calibrate a Spatial Light Modulator and study its optical properties before using the device with synthetic holograms to shape light beams.

Keywords: Spatial Light Modulator (SLM), synthetic holograms.
OCIS codes: (000.0000) General.

References and links

1. "Photonique expérimentale, Optique cohérente." IOGS **SLM,** 35–44 (2024).
2. "Photonique expérimentale, Optique cohérente." IOGS **Annexe : Physique des cristaux liquides,** 45–52 (2024).
3. Chen Jiaqi, Garnier JulienC, "Cahier de manip TP C4, SLM, Séance 3 du 28/11".
4. Vahid Shahabadi, Benjamin Vennes, Ryan Schmedding, Andreas Zuend, Janine Mauzeroll, Steen B. Schougaard, Thomas C. Preston, "Quantifying surface tension of metastable aerosols via electrodeformation," McGill University, Department of Atmospheric and Oceanic Sciences, Department of Chemistry, **Methods,** 7–8, (02 dec. 2024)
5. Ryohei Urata, Hong Liu, Amin Vahdat, "Mission Apollo: Landing Optical Circuit Switching at Datacenter Scale," https://doi.org/10.48550/arXiv.2208.10041 (22 Aug 2022)

1. Introduction

Liquid Cristal Display (LCD) modulate a back-scattering light in order to display a desired pattern onto the screen, resulting in the polarization of the light emitted by the device. While this is a widely used application of liquid cristals, the ability to shape beams are widely used in applied optics. In microscopy, research teams uses Spatial Light Modulators (SLM) to trap aerosols, move them around and even mix aerosols between themselves to study their properties with variating conditions such as humidity, temperature, chemical concentrations [4]. Beam shaping with SLM are used in microscopy to generate self-healing beams, and are also used in telecommunications [5] for optical cross connect devices. SLM are also used in cinematographic projectors and in personnal projector as well.

Spatial Light Modulators are of two types : liquid cristals and MEMs devices such as micromirrors. In this study, we will be working with liquid cristal devices. If MEMs devices can only modulate light in amplitude, liquid cristals can be configured to modulate both amplitude and phase of a lightbeam. Polarization of light is the characteristic that a liquid crystal modifies. A spatial light modulator consists of an array of liquid crystals. Each pixel is controlled by an electric voltage, so each pixel can independently modify the polarization of the light wave passing through it

In the first section of this study, the amplitude modulation, which is usually used for imagery, will be presented; and in the second section, the modulation of the phase which is often used for holography and diffractive imaging, will be presented. At the beginning of this section, a short description of the calibration of the phase modulation will be provided to the reader.

2. Amplitude modulation

In this section, because we work on the modulation of amplitude, we introduce a Laser Speckle Reducer (LSR) before the first polarizer in order to disminish the coherence of the laser beam and smooth the image and the effects of diffractive plate defaults.

Liquid cristals

The following figures illustrate the structure of a liquid crystal pixel; they are taken from the documentation of the Holoeye SLM.

In the absence of applied voltage, the orientation of the molecules follows a helical structure. Between the orientation of the molecules on the input face and that on the output face, the rotation is 90°. Figure 1a illustrates this property.

When a voltage is applied, the orientation of the molecules is altered. Figure b illustrates this effect for three cases. In case (A), no voltage is applied, and the orientation of the molecules rotates while remaining in the plane orthogonal to the propagation axis. In case (B), a non-zero voltage is applied, and the molecules tilt in a direction different from the plane orthogonal to the propagation axis. Finally, in case (C), where a high voltage is applied, the central molecules tilt in the direction of the propagation axis.

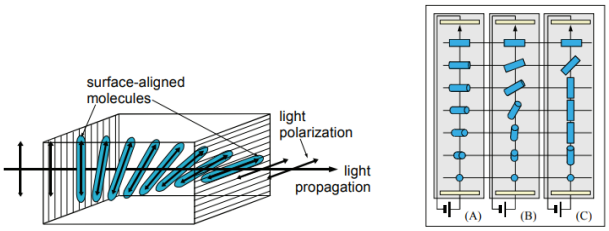

(a) Nematic pixel (b) Effect of voltage

Fig. 1: Nematic pixel principle

The molecules that compose the liquid crystals are anisotropic and confer birefringence properties. Liquid crystals are birefringent materials, generally uniaxial, and thus the ordinary refractive index and extraordinary refractive index are distinguished to describe light propagation within the liquid crystal cell. The controlled orientation of the molecules allows modification of the extraordinary index of the cell, as shown in the principle diagram of Figure 2.

The propagation in the liquid crystal cell can therefore be modeled as a stack of very thin phase plates, with a different orientation as the propagation progresses.

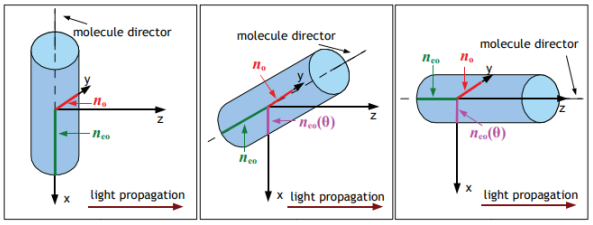

Fig. 2: Nematic pixel indices under input voltage. n_o is the ordinary indice, n_e is the ordinary indice, and n_{ea} is the apparent extraordinary indice

Amplitude calibration

The first step is to measure the "Twist" angle of the SLM, which can be done with a polarizer and an analyzer. Because the light of the laser is already polarized, the first polarizer weaken the amplitude of the incoming laser. In order for the amplitude to remain the same, even when changing the entry polarization, a half-wave plate is added right after the input polarizer (see Fig. 3).

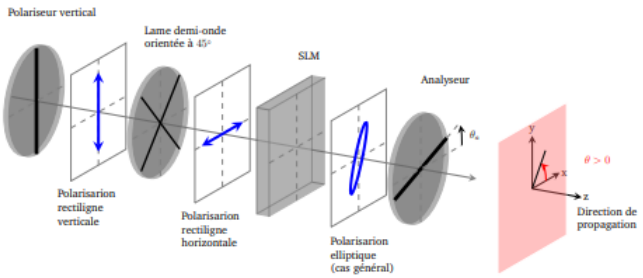

Fig. 3: Calibration system

The effect of a half-wave plate after the polarizer is to introduce a rotation $R = 2\theta$, where θ is the angle between the polarizer and the quarter-wave plate.

With the SLM turned off, and in the configuration $\theta_P = 90°$ and $\theta_{\lambda/2} = -45°$, an extinction is observed for $\theta_A = 0°$, and maximum illumination is observed for $\theta_A = 90°$. The orientation of the half-wave plate $\theta_{\lambda/2} = -45°$ results in a horizontal polarization at the input of the *SLM*, with orientation $R = 90°$. Therefore, the effect of the *SLM* on the polarization is a rotation of $R = -90°$, equal to the "Twist" angle.

With the *SLM* turned on, applying a command of $N_{Right} = 0$ (black) and $N_{Left} = 255$ (white), a contrast inversion is observed on the camera (see Fig.). This indicates that the black command rotates the polarization (by 90°) and the white command corresponds to zero voltage unaffecting the liquid cristals.

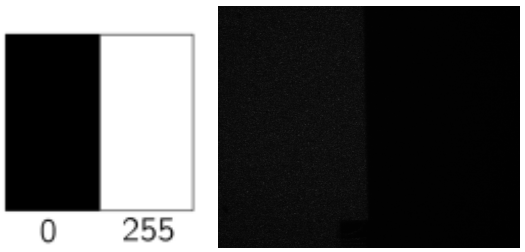

(a) Input command (b) Output (contrast inversion)

Fig. 4: Effect of voltage onto the output figure, before artificial inversion

By rotating the analyzer by 90°, the same pattern as the command is observed. One can also click "inverse command" to get the same effect.

Contrast

The polarizer is still set to $\theta_P = 90°$, with $N_{Right} = 0$ (black) and $N_{Left} = 255$ (white). The analyzer is placed at $\theta_A = 0°$, and the grayscale value on the image is recorded every 10° using "Polarization Analysis": a large rectangle is selected in each zone to average the grayscale level. The intensity received by the camera on the left and right sides is plotted as a function of the angle read on the analyzer.

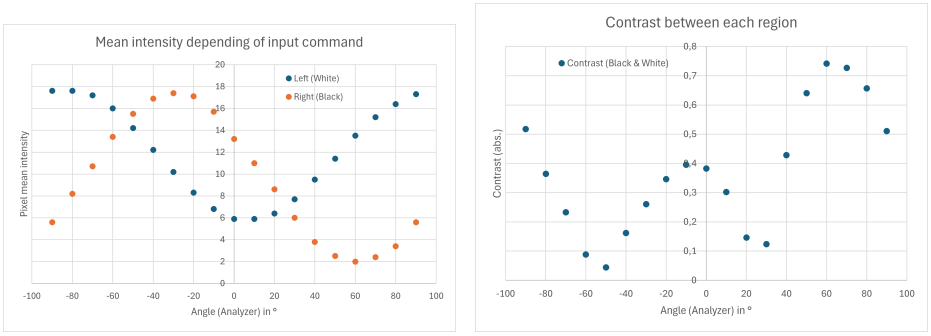

(a) Intensity of each region

(b) Contrast between regions

Fig. 5: Intensity and Contrast resulting of a black and white command

We focus on the amplitude modulation on the left and right sides. The contrast allows us to eliminate the dependency on the integration time. The position of the analyzer axis to achieve maximum contrast is $\theta = 60°$. The position of the polarizer to achieve the brightest image for $N_{Right} = 0$ (black) is 30° (to obtain white on the camera), and for $N_{Left} = 255$ (white) it is $-85°$ (to obtain white on the camera).

The evolution of the intensity, converted into grayscale by the camera, follows a $\cos^2(\theta)$ law. Indeed, Malus' law states that for a polarizer:

$$\frac{I(\theta)}{I_0} = \cos^2(\theta) \tag{1}$$

The *SLM* only rotates the polarization; it acts as a rotator for each pixel. By rotating the analyzer, the intensity variation follows the $\cos^2$ law of a polarizer, where the angle is the one between the analyzer nand the SLM, which is equivalent to the angle between the analyzer and the polarizer (90° introduced twice throughthe half-wave plate and the SLM).

Here, the angle corresponds to the values read on the polarizer and analyzer, using the x-axis as the reference (subtracting 90° would give the polarizer's reference).

Ellipticity

We have:

$$\varepsilon = \arctan\left(\frac{E_{\min}}{E_{\max}}\right) = \arctan\left(\sqrt{\frac{I_{\min}}{I_{\max}}}\right) \tag{2}$$

The polarization at the output of the *SLM* is not linear because there is never total extinction. It is not circular either due to amplitude modulation. The polarization is elliptical, with stronger modulation for $NG = 0$. It is close to being linear on the left side, where the intensity modulation is much more significant than on the right side, resulting in low ellipticity for $NG = 0$.

Command	Black	White
Max Intensity	17,4	17,6
Min Intensity	2	5,9
Ellipticity (rad)	0,32687	0,524826
Ellipticity (°)	18,72829	30,07033

(a) Ellipticity (computed)

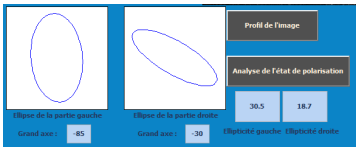

(b) Ellipticity (software)

Fig. 6: Ellipticity measurement

Gray level linearity

The following values are obtained based on the intensity modulation curve from Q4:

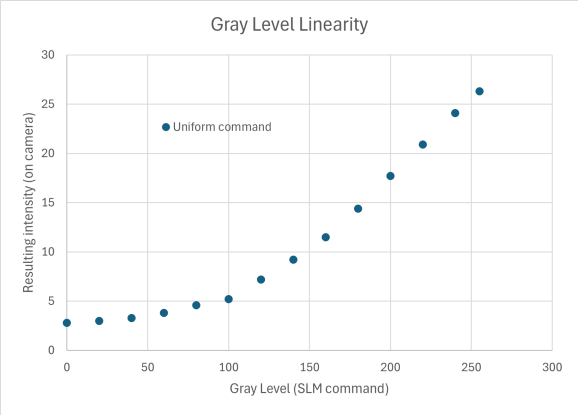

Fig. 7: Linearity of commanded intensity

This time, we position ourselves at $\theta = 60°$, where the contrast is maximal, and then we vary the gray levels from 0 to 255 in steps of 20.

Thus, on both the left and right sides, the response is the same for gray level commands from 0 to 255. There is a correspondence between low and high gray levels for a given exposure time. What interests us is the linearity of the response. The response of the SLM is not linear between the applied and measured gray levels. However, for higher gray levels starting from 140, the response becomes linear.

If the SLM only modified the polarization orientation, we would observe a periodic nonlinear curve, typically corresponding to the square of a sinusoid, depending on the detection based on Malus's law of polarizers.

3. Phase modulation

To observe diffraction, one should remove the Laser Speckle Reducer, to restore the phase of the lightbeam, anbd one should then oberve diffraction produced by defaults of the lens or by dust. The lens L2 should be then placed on the setup so that the Fourier plane is in the detector's plane. We remind that $f_{L2} = 120\,\text{mm}$. Withtout any pattern sent to the SLM, the light interfers with a grating of uniform pitch within horizontal or vertical direction of given pixel pitch pp which is linked to the size of the liquid cristal grating, with different dimensions in the x and y directions, but with a padding that makes every pixel squared.

Diffraction

One can retrieve the pixel pitch with the help of the diffraction formula and the spacing between to bright orders on the detector's plane. We have

$$sin(\theta) = \frac{\lambda}{pp} = \frac{\Delta x}{f'}\Big|_{Fourier\,Plane} \tag{3}$$

Since we measure $\Delta x = 306\,\text{px}$, and since the pixel pitch of the camera is 5,2 µm,we compute a pixel pitch equal to 47 µm. The datasheet provided a value of 32 µm, and we suggest that the difference between the two, above 40%, is due to the padding since the pattern in Fourier's plane is symetric in both x and y directions, as can be seen on Fig. 8a.

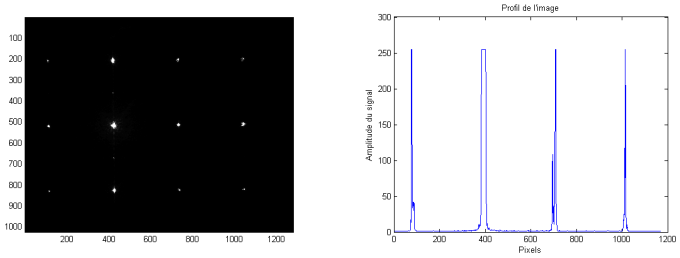

(a) Fourier's plane (b) Horizontal cut

Fig. 8: Measurement of the pixel pitch of the liquid cristal

Phase calibration

We introduce two holes according to Young's experiment after the SLM, and oberve fringed interferences overlayed onto each diffraction orders. We zoom on the brighter, order 0. According to the pattern sent to the SLM, the fringes are horizontally shifted, as can be seen on Fig. 9 from [3].

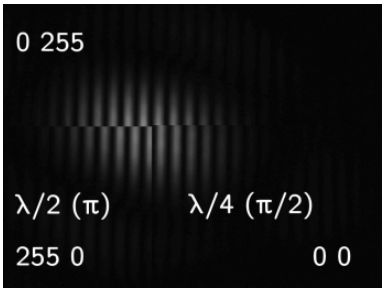

Fig. 9: Phase shift with command input

The SLM changes the phase of the incident lightbeam, acccording to the input command of grey level, and we suppose the relationship between grey level and phase modulation linear. Because we chose the limitation between the blank region (255) and black region (0) between the two holes, one receive light of phase $\varphi_{space} + \varphi_{255}$ while the other receive light with phase $\varphi_{space} + \varphi_0$. We choose the command (0, 255) as the reference. We oberve the shift produced by inversing the command, using (255, 0), which produces a shift of π for the phase, $\lambda/2$ for the optical path difference (OPD). With the intermediate command, using (0, 0), we oberve a shift

of $\pi/2$ for the phase, $\lambda/4$ for the OPD. We thus could use the command (0, 0) as the reference. (We will not in the following)

By running the automated command “Calibration du déphasage”, we can measure the phase shift for a linear shift of grey level of user defined gap. We expect it to be linear and going from 0 rad to 2π rad. Fig. 10 present the result of this measurement.

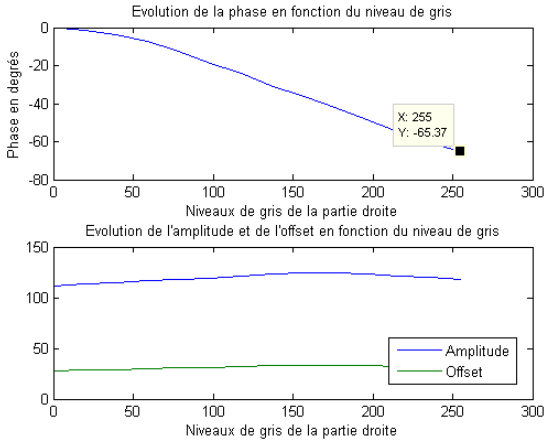

Fig. 10: Linearity of commanded intensity

We observe linearity starting at grey level of 60, and the phase shift only goes from 0 rad to $3\pi/4$ rad approximately. This will produce artifacts in the diffraction produced by the SLM in the case were the input command was computed on the 0 rad to 2π rad range (which is the case when producing synthetic holograms, as can be seen later on)

At this point, it is important to notice that the computed phase shift and OPD are linked to the wavelength of the input laser according to

$$\delta_{OPD} = \frac{2\pi\Delta\varphi}{\lambda} \tag{4}$$

So, with a green laser emitting at 533 nm, the shifts would be larger.

Phase masks

The goal of this subsection is to choose one grating to separate the information between the different orders of diffraction, of a synthetic hologram that will be defined later. We can choose either a rectangular grating or a blased grating. The transmission $t(x) = \mathrm{e}^{-j\Phi(x)}$ of the grating is periodic and can be expressed as a convolution product with a Dirac comb:

$$t(x) = (m \star \mathrm{III}_p)(x)$$

where the elementary pattern is denoted $m(x)$. This results in a series of bright points spaced proportionally to $\frac{1}{P}$.

Blased mask

The intensity of each bright point, i.e., each diffraction order k, is proportional to the coefficient A_k:

$$A_k = \left| \frac{1}{P} \tilde{m}\left(\frac{k}{P}\right) \right|^2 = \left| \frac{\sin\left(\frac{\Phi_M}{2} + \pi k\right)}{\frac{\Phi_M}{2} + \pi k} \right|^2$$

If the modulation depth is less than 2π, the measurement of respectively, order 0 an order 1:

$$A_0 = \left| \frac{\sin\left(\frac{\Phi_M}{2}\right)}{\frac{\Phi_M}{2}} \right|^2 \qquad A_1 = \left| \frac{-\sin\left(\frac{\Phi_M}{2}\right)}{\frac{\Phi_M}{2} + \pi} \right|^2$$

can allow retrieving the value of Φ_M.

In the case of a phase mask created by an SLM, the phase shift profile is modified by pixelation. For example, instead of a linear phase shift, steps are obtained. This time, the elementary pattern, named $n(x)$ can be expressed from the previous pattern $m(x)$ as:

$$n(x) = \left((m \cdot \mathrm{III}_L) \star \mathrm{Rect}_L \right)(x)$$

The diffraction pattern will thus correspond to that of the continuous grating, periodicized and modulated by $\left|\widetilde{\mathrm{Rect}_L}(\nu)\right|^2$, as can be seen on Fig. 11a.

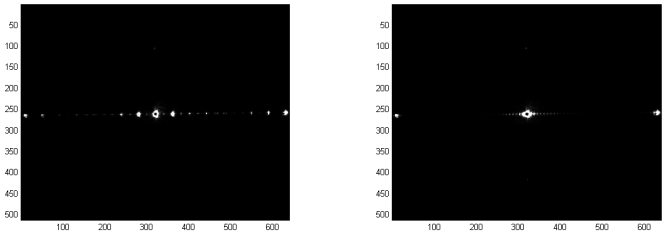

(a) Blased mask, gap 5 (b) Blased mask, gap 20

Fig. 11: Diffraction produced by blased masks

Because the available range for the phase is only $[0, 3/\pi/4]$, we observe artifacts located around the diffraction orders 0 and ± 1. The more important the gap, the closer the diffraction orders. Indeed, their spacing is proportional to the inverse of the gap.

Rectangular mask

As detailed in the Annexe section, the first term in the expression of $\tilde{m}(\nu)$ is null for even values of k, except 0. For odd terms, the magnitude of this first term equals $\frac{P}{k\pi}$:

$$A_k = \frac{2}{k^2\pi^2} \cdot (1 - \cos(\Phi_M))$$

The coefficient corresponding to order 0 has the expression:

$$A_0 = \left(\cos\left(\frac{\Phi_M}{2}\right) \right)^2 = \frac{1}{2}(1 + \cos(\Phi_M))$$

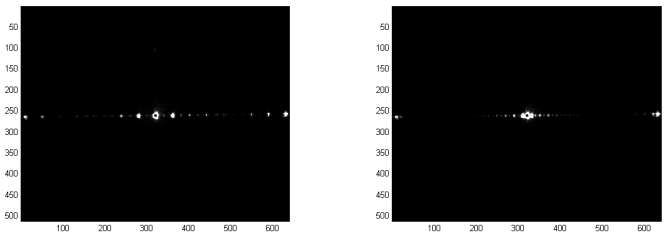

(a) Squared mask, gap 5 (b) Squared mask, gap 20

Fig. 12: Diffraction caused by rectangular masks

For a maximal phase shift of $\Phi_M = 2\pi$, only order 0 is non-zero. Conversely, for a phase shift depth $\Phi_M = \pi$, order 0 is null. Because the SLM modulates the phase approximately between 0 and $\pi/2$ rad the blased grating is more appropriate. Indeed, in the theoretical case where the phase could be modulated form 0 to 2π, we would oberve very bright intensity on the order -1 for the balsed mask and 0 for the rectangular one, thus we will choose the blased mask for separating the information. Moreover, the rectangular mask would introduce more artifacts, due to its large harmonic constituents, that would decrease the quality of the separation here with a SLM blocked to $[0, 3/\pi/4]$ in phase modulation.

In the end, because the camera is only sensing intensities, and because we know that $I \propto |E|^2 = |A(\sigma,\mu) \times exp(i\Phi(\sigma,\mu))|^2 = A^2$, the information of the phase is lossed, but its role in separating the different orders is still useful.

Synthetic holograms

Thanks to Gerchberg-Saxton's algorithm that codes a picture (Fig. 14a) into a phase mask (Fig. 13a) that will reconstruct the picture in Fourier's plane after illuminating the mask with a coherent lightbeam, we can encode a particular image and study its reconstruction using the SLM as the physical mask.

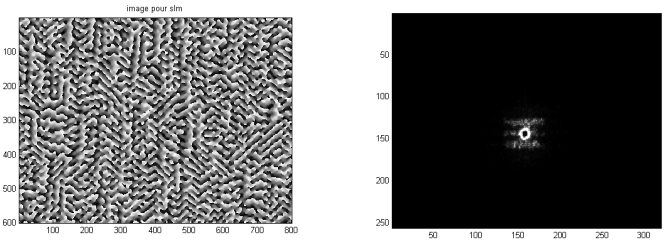

(a) Gerchberg-Saxton's encoding (b) Fourier's plane

Fig. 13: Reconstruction of a picture

We obtain Fig. 13b on which the reconstructed picture is duplicated between order =1 and -1 and overlayed. We thus introduce a blased grating through a convolution with the output of Gerchberg-Saxton's algorithm and obtain Fig. 14b [3].

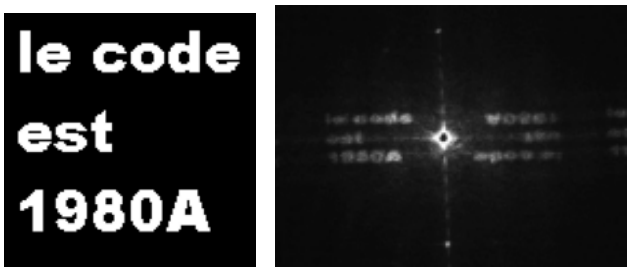

(a) Original picture (b) Fourier's plane (shifted)

Fig. 14: Reconstruction of a picture (shifted)

4. Conclusion

The ultimate goal of this study was to reconstruct the image of a picture encoded with Gerchberg-Saxton's algorithm onto a Spatial Light Modulator. To do that, we have first established the behavior of the liquid cristal SLM used, and particularly the way it changes the polarization of light, working with amplitude modulation. We ultimately computed the ellipticity of the output light. Then we studied the SLM in terms of phase modulation, and computed the pixel pitch of the liquid cristals thanks to the diffraction formula. We calibrated the SLM in terms of phase modulation for a given grey level command, and understood the impact of phase modulation total range on the influence of artifacts on the final image, and the role of gratings to separate overlayed duplicated images between diffraction orders. The study of two types of gratings, rectangular and blased, ultimately allowed to choose the blased one to separate the two diffracted reconstructed images of the original picture.

List of Figures

5. Annexe

The transmission $t(x) = \mathrm{e}^{-j\Phi(x)}$ of the grating is periodic and can be expressed as a convolution product with a Dirac comb:

$$t(x) = (m \star \mathrm{III}_p)(x)$$

where the elementary pattern is denoted $m(x)$.

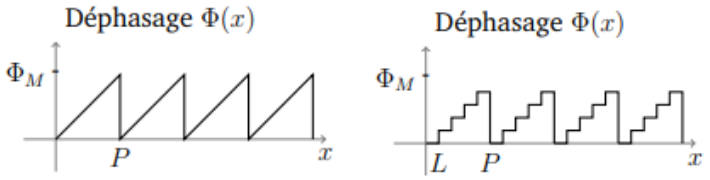

(a) Ellipticity (computed) (b) Ellipticity (software)

Fig. 15: Ellipticity measurement

Diffraction by such a grating allows obtaining, in the Fourier plane, a field proportional to the Fourier transform of the grating, which can be expressed, limiting to a single direction ν, as:

$$\tilde{t}(\nu) = \frac{1}{P} \cdot \tilde{m}(\nu) \cdot \mathrm{III}_{\frac{1}{P}}(\nu)$$

This results in a series of bright points spaced proportionally to $\frac{1}{P}$. The intensity of each bright point, i.e., each diffraction order k, is proportional to the coefficient A_k:

$$A_k = \left| \frac{1}{P} \tilde{m}\left(\frac{k}{P}\right) \right|^2$$

In the case of the grating shown in Figure 4.9, the expression of the Fourier transform $\tilde{m}(\nu)$ of the pattern $m(x)$ is given by:

$$\tilde{m}(\nu) = \int_0^P \mathrm{e}^{-j\frac{\Phi_M}{P} \cdot x} \cdot \mathrm{e}^{-j2\pi\nu x}\, dx$$

This Fourier transform can be rewritten as a dilated and shifted sinc function:

$$\tilde{m}(\nu) = P\mathrm{e}^{-j\frac{\Phi_M}{2}} \cdot \mathrm{e}^{-j\pi\nu P} \operatorname{sinc}\left(P\left(\frac{\Phi_M}{2\pi P} + \nu\right)\right)$$

The intensities of the different diffraction orders k are then proportional to:

$$A_k = \left| \frac{\sin\left(\frac{\Phi_M}{2} + \pi k\right)}{\frac{\Phi_M}{2} + \pi k} \right|^2$$

If the modulation depth is less than 2π, the measurement of order 0:

$$A_0 = \left| \frac{\sin\left(\frac{\Phi_M}{2}\right)}{\frac{\Phi_M}{2}} \right|^2$$

of order 1:

$$A_1 = \left| \frac{-\sin\left(\frac{\Phi_M}{2}\right)}{\frac{\Phi_M}{2} + \pi} \right|^2$$

can allow retrieving the value of Φ_M.

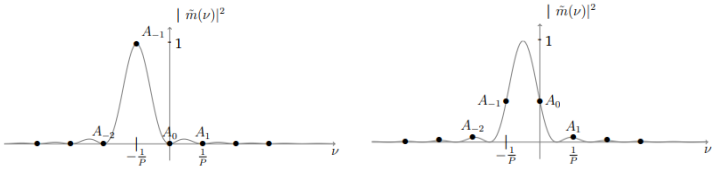

(a) Ellipticity (computed) (b) Ellipticity (software)

Fig. 16: Ellipticity measurement

In the case of a phase mask created by an SLM, the phase shift profile is modified by pixelation. For example, instead of a linear phase shift, steps are obtained, as shown in Figure 4.12.

The transmission $t(x) = \mathrm{e}^{-j\Phi(x)}$ of the grating remains periodic and can be expressed as a convolution product with a Dirac comb:

$$t(x) = (n \star \mathrm{III}_P)(x)$$

where the elementary pattern $n(x)$ can be expressed from the previous pattern $m(x)$ as:

$$n(x) = ((m \cdot \mathrm{III}_L) \star \mathrm{Rect}_L)(x)$$

where the rectangle function $\mathrm{Rect}_L(x)$ is defined as:

$$\mathrm{Rect}_L(x) = \begin{cases} 1 & \text{if } x \in [0, L] \\ 0 & \text{otherwise} \end{cases}$$

The Fourier transform of the pattern $n(x)$ can thus be written as:

$$\tilde{n}(\nu) = \left(\tilde{m} \star \frac{1}{L}\mathrm{III}_{\frac{1}{L}}\right)(\nu) \cdot \widetilde{\mathrm{Rect}_L}(\nu)$$

The diffraction pattern will thus correspond to that of the continuous grating, periodicized and modulated by $\left|\widetilde{\mathrm{Rect}_L}(\nu)\right|^2$. In the case of a modulation depth equal to 2π, the diffraction orders are represented in Figure 4.13.

Rectangular Mask

$$\begin{aligned} \tilde{m}(\nu) &= \int_0^{\frac{P}{2}} \mathrm{e}^{-j\Phi_M} \cdot \mathrm{e}^{-j2\pi\nu x}\, dx + \int_{\frac{P}{2}}^{P} \mathrm{e}^{-j2\pi\nu x}\, dx \\ &= \frac{-\left[\mathrm{e}^{-j\pi\nu P} - 1\right]}{j2\pi\nu} \cdot \mathrm{e}^{-j\Phi_M} \cdot \mathrm{e}^{-j\pi\nu\frac{P}{2} + j\frac{\Phi_M}{2}} \left[2\cos\left(-\pi\nu\frac{P}{2} + \frac{\Phi_M}{2}\right)\right] \end{aligned}$$

The first term in the expression of $\tilde{m}(\nu)$ is null for even values of k, except 0. For odd terms, the magnitude of this first term equals $\frac{P}{k\pi}$:

$$A_k = \left| \frac{1}{k\pi} \cdot \left[2\cos\left(-\frac{k\pi}{2} + \frac{\Phi_M}{2} \right) \right] \right|^2$$

$$A_k = \frac{2}{k^2\pi^2} \cdot (1 - \cos(\Phi_M))$$

To calculate order 0, the first term in the expression of $\tilde{m}(\nu)$ must be expressed:

$$\frac{-\left[\mathrm{e}^{-j\pi\nu P} - 1 \right]}{j2\pi\nu} = \mathrm{e}^{-j\frac{\pi\nu P}{2}} \cdot \frac{P}{2} \cdot \frac{\sin\left(\frac{\pi\nu P}{2}\right)}{\frac{\pi\nu P}{2}}$$

The magnitude of this first term equals $\frac{P}{2}$ for $\nu = 0$. The coefficient corresponding to order 0 has the expression:

$$A_0 = \left(\cos\left(\frac{\Phi_M}{2} \right) \right)^2 = \frac{1}{2}(1 + \cos(\Phi_M))$$

For a maximal phase shift of $\Phi_M = 2\pi$, only order 0 is non-zero. Conversely, for a phase shift depth $\Phi_M = \pi$, order 0 is null.